International Journal of MC Square Scientific Research Vol.8, No.1 Nov 2016

Impedance Source Based Multi Phase Inverter Fed Variable Speed PMBLDC Motor Using Advance controller for Torque Ripple Minimization

M. Simon Darsingh
Research Scholar
Department of EEE, Maharishi University of Information Technology, Lucknow, Uttar Pradesh.
Email: simonphd123@gmail.com

Dr. Sanjay S Chaudhary
Asst Professor
Department of EEE, Maharishi University of Information Technology, Lucknow, Uttar Pradesh.

Abstract - This paper presents the advance controlling system for multiphase PMBLDC motor. This permanent magnet synchronous motor has copper losses in stator, current vibration and harmonics due to wrong selection of rotor shape is generated by the voltage saturation and more torque ripple. This voltage saturation affects the performance of the motor. The proposed multiphase permanent magnet BLDC motor is to reduce the voltage saturation and also to minimize the torque ripple. The multiphase motor have more handling capacity, high reliability and to produce high torque at same ampere volume of machine. This multiphase topology is requiring high dc source and effective control method for high speed operation. The introduced Z-source topology is used to improve source voltage boost up ability without using any DC/DC converters. Further, it reduces the line harmonics, enhance the load power factor, gives ride through ability in the course of input voltage sags and increases inverter reliability. The IFOC control strategy is possible to achieve high reliable operation at input voltage sag conditions. The proposed Z-source networks as well as IFOC scheme based multi phase motor to attain the minimum torque ripples and high voltage gain in ASD (adjustable speed drive) are analyzed in MATLAB/ SIMULINK environment.

Keywords - Multi Phase, torque ripple, voltage saturation, PMSM, ZSI, IFOC, ASD (adjustable speed drive), vector control, and variable speed drives.

1. Introduction

The trapezoidal permanent magnet brushless dc motor is associated with corresponding multiphase inverter [1]. Number of legs in the inverter should be equal to the number of stator windings of the motor and the commutation is accomplished by electronic switches (IGBT). Permanent magnet synchronous motor (PMSM) drives can be used in all kinds more attractive in motion control applications such as High Speed Trains and electric vehicles. The main features and advantages are followed: high efficiency, good performance, low inertia ratio, high torque-to-volume ratio, good power factor, which is compared to induction and reluctance motors, PMSM has achieved high density and small size [2-3]. The voltage source inverter is made by using power electronic switches; varies control strategies are followed: PWM, SPWM, SVPWM etc., [4-6], the traditional z source

inverter is shown in fig.1. The dc source is located with two side of z source inverter [7-9]. The leg switching arrangement controlled by using PI control strategy; L_1 , L_2 have same Inductor current ripples. But given input source is not enough for motor operation the conventional Z-source topology is also operated under various shoot through condition.

A PMSM is produce the air gap magnetic field rather than using electromagnets. the multiphase PMSM is proposed in this paper; which have more advantages over traditional three phase drives, the multi phase PMSM is used to increases the frequency of pulsating torque, also decreased the torque pulsations, reduced the current harmonics, improved the phase voltage as well as torque/current relation for the same volume of the drive [10-14]. Those are applicable in high power applications, such as electric/hybrid vehicles, aerospace application, warship, submarine propulsion and circulation pumps in nuclear power plants.

Additionally, Z source inverter is very suitable replacement for traditional VSI and CSI. Z source inverter is very simple to explain two ports and x shape LC network between input and inverter voltage.[15] With sole network LC network, we can purposely add the shoot through state to boost output voltage level. Using this method, we can get higher or lower level voltage.

Therefore, voltage gain capability decreased and potential stress occurred on Z-source capacitor; low voltage gain and mechanical stresses to create a current harmonics in rotor side; therefore the conventional system can produce poor motor performance. Since PWM control scheme is not suitable for high speed operation. The proposed impedance network is developed to improve input voltage boost ability. Since it requires small shoot through duty ratio for voltage gain and proposed to reduce the voltage stresses [16-17].

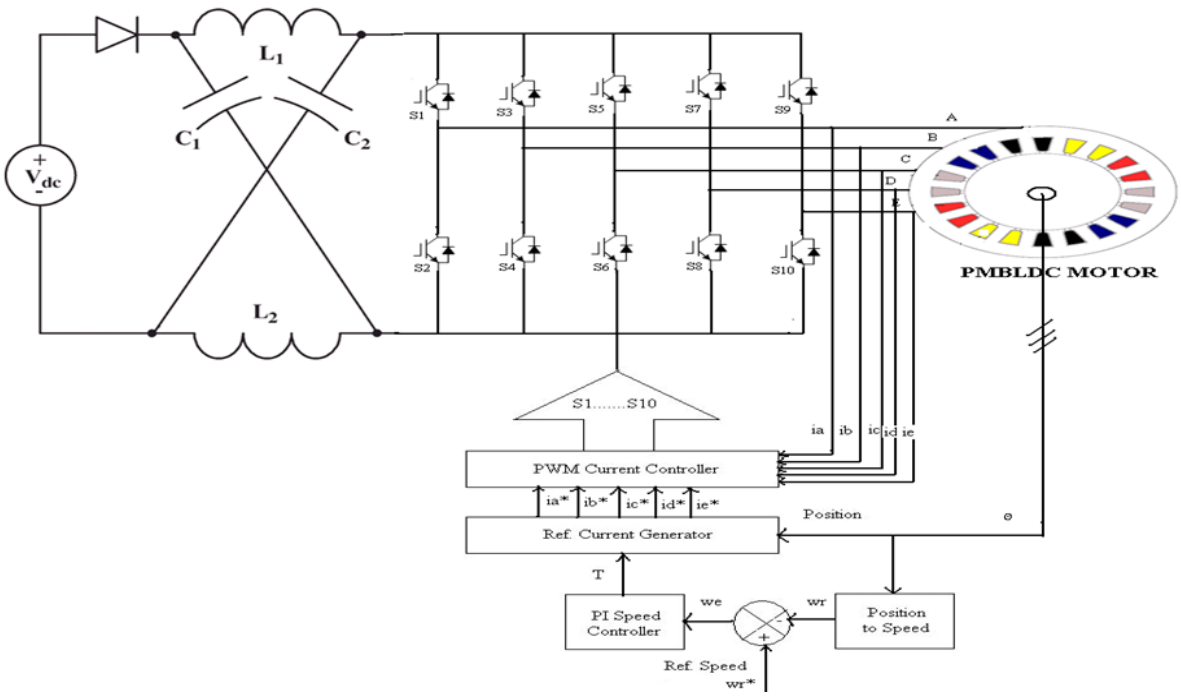

Fig. 1 Conventional Circuit Diagram

Multiphase inverter required standard control techniques; compared with other control methods, IFOC algorithm is only suitable for handling the dynamic and variable load

application. In IFOC control method has rotor flux vector, which is implemented by using the field oriented vector control equations, is required the rotor speed. The PMSM is required to operate at a rated torque with speed control to improve energy efficiency. In fact, the back-EMF and motor speed of the PMSM is proportional and the developed torque(Tm) is proportional to its phase current (I). Therefore, a rated torque is maintained by a constant current in the stator of the five phases motor.

The proposed five-phase IFOC based ZSI system that provides higher reliability, better dynamic performance, higher efficiency. Additionally, ZSI topology is evaluated and proposed to achieve boost voltage gain without using any dc to dc converter. This paper proposes a detailed modeling, design and result evaluation of IFOC strategy based multiphase PMSM drive for fast dynamics operation of torque ripple minimization. Different torque at various speed conditions is achieved in MATLAB/Simulink environment.

2. General Descriptions

2.1 Modeling of Five Phases PMSM

The five phases PMSM model is derived from three phase PMSM. The proposed five-phase PMSM is the smallest commonly used phase variable based multiphase motor. Therefore n number of phases is considered in PMSM; where 'n' is the no of phases that is derived from (360˚/n). It processes five phase stator windings are displaced with a phase difference of 72˚ degree for all individual phases [11]. By increasing the number of phases in stator side, the machine has produced the lower space harmonic content in field. Hence the efficiency is also high; in multiphase inverter fed PMSM has equal stator windings and number of phase [14], [15].

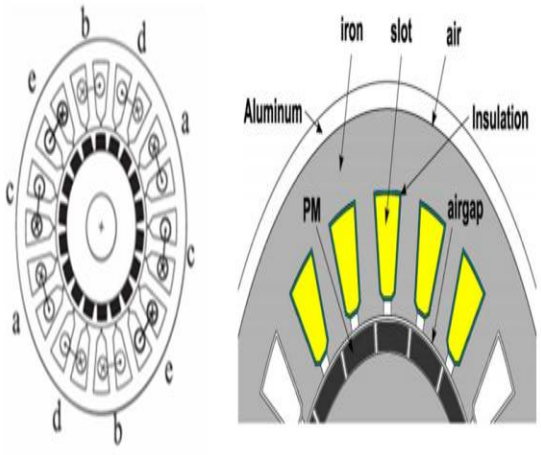

Fig. 2 FE model of the five-phase motor

The proposed PMSM model is described by using 20-slots 18-poles which is shown in fig.2. The proposed motor has been designed to obtain a high speed and transient torque and also maintain the fault-tolerance capability.

Fig.3. shows the phasor diagram of the phase to neutral voltage, V_{AN} is taken as reference and the phase sequences which is considered at 72˚.

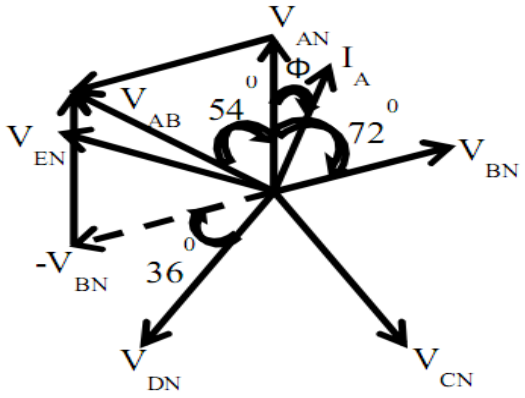

Fig. 3 phasor diagram

The steady-state voltage equations of a five-phase -PMSM in the rotor reference frame and abcde transformation can be written as follows

Stator voltage is derived as in equation 1,

$$V_S = R_S I_S + \rho \lambda_S \quad (1)$$

Air-gap flux linkages are presented by equation 2,

$$\lambda_S = \lambda_{SS} + \lambda_m \quad (2)$$

Substitute the flux linking stator winding currents in the stator windings in terms of the stator winding inductances,

$$\lambda_S = L_{SS} i_S + \lambda_m \quad (3)$$

L_{ss} Is the stator inductance matrix which can contains the self and mutual inductances of the stator phases, from the above equation3, R_S , I_S , λ_S are the stator resistance, current, flux linkages matrices respectively.

$$V_S = [V_a V_b V_c V_d V_e]^T \quad (4)$$

$$I_S = [I_a I_b I_c I_d I_e]^T \quad (5)$$

From equation 6, the matrix value of the stator inductances are given by $\alpha = \frac{2\pi}{5}$

$$L_{ss}=\begin{bmatrix} L_{aas} & L_{abs} & L_{acs} & L_{ads} & L_{aes} \\ L_{bas} & L_{bbs} & L_{bcs} & L_{bds} & L_{bes} \\ L_{cas} & L_{cbs} & L_{ccs} & L_{cds} & L_{ces} \\ L_{das} & L_{dbs} & L_{dcs} & L_{dds} & L_{des} \\ L_{eas} & L_{ebs} & L_{ecs} & L_{eds} & L_{ees} \end{bmatrix} \qquad (6)$$

Arbitrary transformation is introduced into the phase variable into rotating arbitrary angularly velocity. The transformed matrix is following;

$$k_s=\begin{bmatrix} \cos\theta_\gamma & \cos\left(\theta_\gamma-\frac{2\pi}{5}\right) & \cos\left(\theta_\gamma-\frac{4\pi}{5}\right) & \cos\left(\theta_\gamma+\frac{4\pi}{5}\right) & \cos\left(\theta_\gamma+\frac{2\pi}{5}\right) \\ \sin\theta_\gamma & \sin\left(\theta_\gamma-\frac{2\pi}{5}\right) & \sin\left(\theta_\gamma-\frac{4\pi}{5}\right) & \sin\left(\theta_\gamma+\frac{4\pi}{5}\right) & \sin\left(\theta_\gamma+\frac{2\pi}{5}\right) \\ \cos\theta_\gamma & \cos\left(\theta_\gamma-\frac{4\pi}{5}\right) & \cos\left(\theta_\gamma-\frac{2\pi}{5}\right) & \cos\left(\theta_\gamma+\frac{2\pi}{5}\right) & \cos\left(\theta_\gamma-\frac{4\pi}{5}\right) \\ \sin\theta_\gamma & \sin\left(\theta_\gamma+\frac{4\pi}{5}\right) & \sin\left(\theta_\gamma-\frac{2\pi}{5}\right) & \sin\left(\theta_\gamma+\frac{2\pi}{5}\right) & \sin\left(\theta_\gamma-\frac{4\pi}{5}\right) \\ \frac{1}{\sqrt{2}} & \frac{1}{\sqrt{2}} & \frac{1}{\sqrt{2}} & \frac{1}{\sqrt{2}} & \frac{1}{\sqrt{2}} \end{bmatrix} \qquad (7)$$

From equation 7, transformation matrix $\theta_\gamma=0$

$[K_S]^{-1}$ Is derived from pseudo orthogonal property, is given in equation 8,

$$[K_S]^{-1}=\frac{5}{2}[K_S] \qquad (8)$$

Voltage equation (10) gets from transformation matrix which is multiplied with equation (1)

$$[K_S]V_S=[K_S]R_S I_S+[K_S]\rho\lambda_S \qquad (9)$$

$$V_{qdxyo}=[K_S]R_S[K_S]^{-1}I_{qdxyo}+[K_S]\rho[K_S]^{-1}\lambda_{qdxyo}+\lambda_{qdxyo} \qquad (10)$$

$$L_{qdxyo}=\begin{bmatrix} L_q & 0 & 0 & 0 & 0 \\ 0 & L_d & 0 & 0 & 0 \\ 0 & 0 & L_x & 0 & 0 \\ 0 & 0 & 0 & L_y & 0 \\ 0 & 0 & 0 & 0 & L_0 \end{bmatrix} \qquad (11)$$

$$L_d=L_{ls}+L_m \qquad (12)$$

$$L_q=L_{ls}+L_m \qquad (13)$$

$$\lambda_m=\begin{bmatrix} \lambda_m \\ 0 \\ 0 \\ 0 \\ 0 \end{bmatrix} \qquad (14)$$

$$V_q=R_S I_q+\rho\lambda_q+\omega\lambda_m+\omega L_d I_q \qquad (15)$$

$$V_d=R_S I_q+\rho\lambda_{dq}-\omega L_d I_q \qquad (16)$$

$$V_x = R_s i_x + \rho L_{ls} \quad (17)$$

$$V_y = R_s i_y + \rho L_{ls} \quad (18)$$

$$V_0 = R_s i_0 + \rho L_{ls} \quad (19)$$

Where λ is the inertia and ρ is the number of poles pairs

2.2 Five-Leg Inverter

Generally the multiphase (more than three phases) motors considered for high speed applications due to their inherent advantages compared with three phase drives. The multiphase inverter electric drive is limited to the controlling of the supply system. In fact it can be able to develop any static transformation system to change the phase number from three to n-phases. Five-phase VSIs covers single and three phase power applications. The main advantage of these five phase scheme is to provide always controllable and rated phase amplitude, and frequency. PMSM drive system requires sinusoidal voltage waveform. Therefore the five-phase VSI topology is operated as per the switching table. 1.

From this; the five phase power is derived as,

$$P = 5V_{ph}I_{ph}\cos\phi \text{ Or } P = 4.25V_L I_L \cos\phi \quad (*)$$

Therefore, the five-phase power is greater than three-phase power, whereas five-phase power is 2.52 times greater than three-phase power and 4.25 times greater than the single-phase power.

Table. 1 Switching Format

Angle / Degree	Leg 1	Leg 2	Leg 3	Leg 4	Leg 5
0°	$S1$	$S8$	$S10$	$S7$	$S9$
36°	$S1$	$S8$	$S10$	$S2$	$S9$
72°	$S1$	$S3$	$S10$	$S2$	$S9$
108°	$S1$	$S3$	$S10$	$S2$	$S4$
144°	$S1$	$S3$	$S5$	$S2$	$S4$
180°	$S1$	$S3$	$S5$	$S2$	$S4$
216°	$S6$	$S3$	$S5$	$S2$	$S4$
252°	$S6$	$S8$	$S5$	$S7$	$S4$
288°	$S6$	$S8$	$S5$	$S7$	$S9$
324°	$S6$	$S8$	$S10$	$S7$	$S9$
360°	$S6$	$S8$	$S10$	$S7$	$S9$

2.3 Torque Ripple Minimization

At first, surface of the PMSM permanent magnet is enclosed with the smooth surface of the rotor inductance value of the d&q-axis are same. However the relative permeability of a permanent magnet is nearly equal to the air gap of the magnetic path. From the fig.4 the d-axis differs from q-axis inductance. Magnetic flux occurs in d-axis so q-axis inductance is greater than d-axis. The reluctance torque is generated by magnetic saliency from the several of inductance.

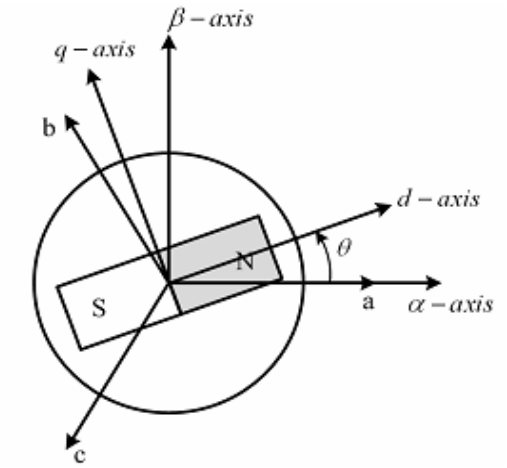

Fig. 4 d&q-axis reference diagram.

Accordingly, the generated torque of the PMSM consists of the magnetic torque and the reluctance torque as followed in equation (20)

$$T_e = \left(\frac{5}{2}\right)\left(\frac{p}{2}\right)\{\lambda_d i_q - \lambda_q i_d\} \qquad (20)$$

Therefore many pairs of d&q axis current can be generated in same rated torque condition.

3. Impedance Source Inverter

The traditional voltage-source inverter serves as buck type (step down) converter, a rectifier front end diode and dc link capacitor arrangements are used to achieve good output voltage with low harmonic levels. But VSI can have more disadvantages; such as limited output voltage and the unregulated source voltage. Therefore, dc to dc boost converter is required. The proposed z-source inverter acts as a buck-boost converter without using of additional switches, which is obtained from wide range of desirable output voltage [7]. The proposed topology reduces the voltage stresses of capacitors, power devices and diodes for the same input and output voltage. Furthermore it can improve the conversion boost up efficiency and which is overcomes the voltage limitation of the conventional VSI, CSI and also has several special features [9-10]. A mono stage structural inverter can produce required buck and boost output voltage.

Highly increases the inverter reliability. There is no dead time; since perfect sinusoidal output waveform is achieved. In proposed z-source network, the minimized size of the Z-source capacitors are used improve the ZSI topology. Currently, two improved ZSI topologies are presented [8], called as the embedded and series ZSI, respectively. Which is proposed topology can decrease the size and cost of the capacitor and improves the power density. Where the DC source is series connected with the inductor in proposed series ZSI network, five phase inverter and input source are connected at two sides of the Z-source network [12]. Modulation strategy and inductor current are exactly same for both embedded and series ZSI topology is derived following equation [13]

$$V_c = \frac{D_{sh}}{1-2D_{sh}} V_{dc} \tag{21}$$

$$V_c = 2V_c + V_{dc} = \frac{D_{sh}}{1-2D_{sh}} V_{dc} \tag{22}$$

Where, D_{dc} - Dc source voltage, D_{sh} - Shoot-through duty ratio.

In the shoot-through state the inductors are charged and the capacitors are discharged, the energy will be transferred through the power source to the inductor, where the inductor current is described as

$$\frac{di_L}{dt} = \frac{V_{dc}+V_c}{L} = \frac{(1-D_{sh})v_i}{L} \tag{23}$$

Where, i_L - Inductor current, L – Inductance.

In the non-shoot-through state the inductor is discharged; the capacitor is charged, the energy is transferred from the power source to the load.

4. IFOC Control Structure

High performance and dynamic load applications based multiphase drives required special control algorithms. Fig.5 illustrates the control structure of IFOC scheme which is based on PMSM drive considered in this investigation [3]. As the proposed drive consists of z-source with five phase inverter switching arrangements, the most common vector principle independently controls the torque and flux in PMSM. In the indirect field oriented control method, different type of co-ordinate transformation has produce stator voltage or stator current in rotating reference frame at the angular velocity. The d&q axis are responsible for stator current produced torque and flux. [8]-[9] Those field and torque currents are orthogonal with two vector axis (d&q). Q-axis reference current i_{qs}^* is may be computed by using the reference torque, is given in equation 24,

$$i_{qs}^* = \frac{2}{5}\frac{2}{p}\frac{L_r}{L_m}\frac{T_{ref}}{\psi_r} \tag{24}$$

Where ψ_r is rotor flux, which is derived in equation 25,

$$\psi_r = \frac{L_m}{\tau_r s + 1} i_{ds} \qquad (25)$$

Where, L_m - Magnetization inductance, L_r - Rotor inductance, τ_r -rotor time constant.

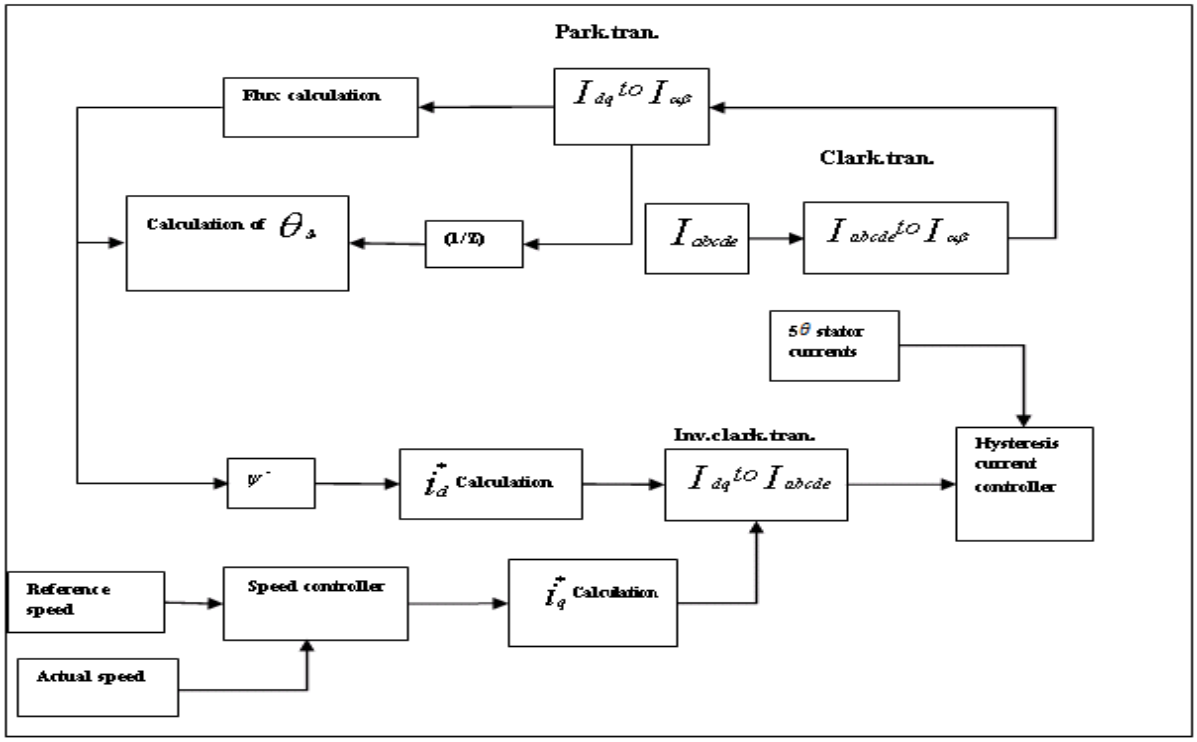

Fig. 5 block diagram for IFOC topology

D-axis referred stator reference current $i_{ds}*$ is derived in equation 26,

$$i_{ds}* = \frac{\psi_{ref}}{L_m} \qquad (26)$$

By using the rotor speed ω_r ,the slip frequency ω_{sl} , which is given in equation 27,

$$\omega_{sl} = \frac{1}{\tau_\gamma} \frac{i_{ds}*}{i_{qs}*} \qquad (27)$$

Angle of the rotor flux θ_ϑ is derived in equation 28,

$$\theta_\vartheta = \int (\omega_{sl} + \omega_r) dt \qquad (28)$$

5. Switching-Tables Based State Of Operation

The proposed speed control loop described in multiphase system. In this section detailed simulation studies have been performed initially in order to fully develop the control strategy. Here, the results are compared with conventional system. The concept of commutated linear

equivalent circuits was applied to the machine, i.e., every 〖72〗^° electrical degrees two equivalent circuits valid for forced and freewheeling conditions are shown in fig:3.therefore the five phase motor have been operated in 〖72〗^° angle difference and each switch has commutated at 〖36〗^°. The state of switching operation fully depends on the table 1

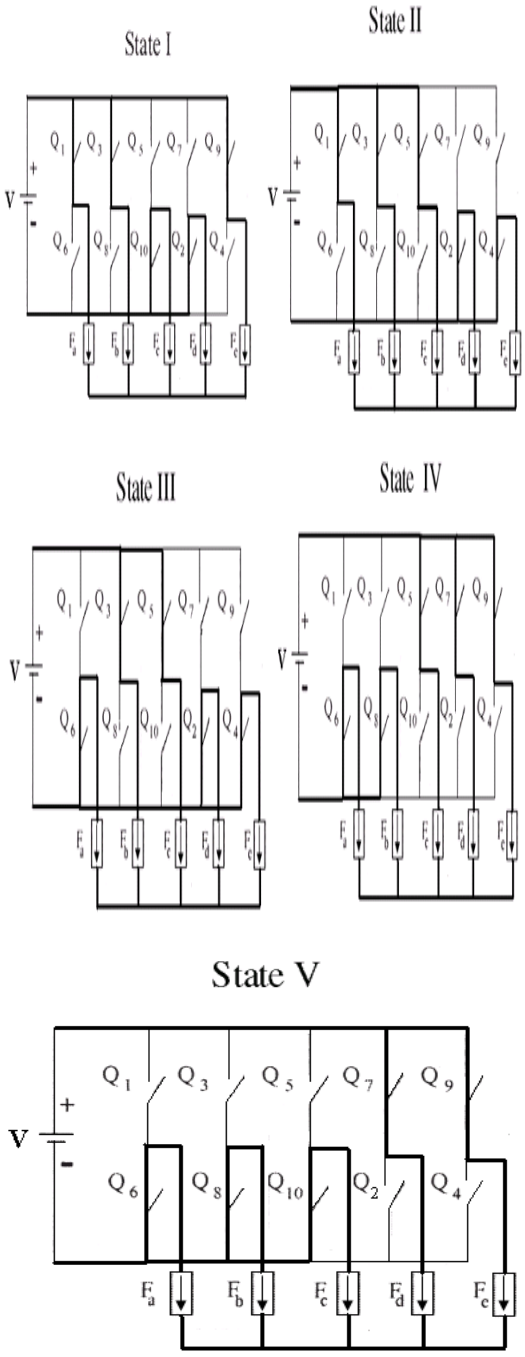

Fig. 6 five phase operating state diagram; state I: 72°; state II: 144°; state III: 216°; state IV: 288°; state V: 360°.

Fig.6 shows the switch operating states at five phase angles ($72^{\circ}, 144^{\circ}, 216^{\circ}, 288^{\circ}, 360^{\circ}$) state:1 the motor operated at angle of 72° is shown in Fig4. The following are the assumptions. Conduction starts from phase A, the switches Q1, Q3, Q9, and, Q10, Q2 are commutated. Initially the Q1, Q3, Q9 switches are allows +ve current flow and Q10, Q2 are –ve conduction. , impressing excitation for phases A, B,C,D and E, while there is still current flowing on the machine coils due to the last driving stage as indicated by the free-wheeling path. Such an approach is applied subsequently to all the remaining phases. Retrieving the currents derived from all those difference states. Where the current harmonic in rotor is the other important issues were found for accurate machine mathematical modeling.

Moreover, the mutual inductance between phases and armature reaction can be occurs as distortion in existing brushless dc-machines. Additionally the conventional topology should require one phase with null current every time. But recent trend requires fourth order system, while a fifth phase is not kept off condition. However, each phase are permitting the dynamic operation and each stage has its own current, equivalent back emf. The induced voltage due to the changing emf delivers mechanical energy. Thus, the ripple less pure form of torque should be induced in five-phase BPM machine has to account for the air- gap flux distortion by the armature reaction

6. Simulation Results

The proposed estimation method was demonstrated by using the MATLAB software. The overall performance of the proposed PMBLDC drive system operation is shown in Fig.7 (a,b,c) shows overall simulation circuit and respective IFOC controller part. The simulation parameters are given in table.2. The indirect field oriented current and speed control included in the drive system is fed from dc link voltage impedance network.

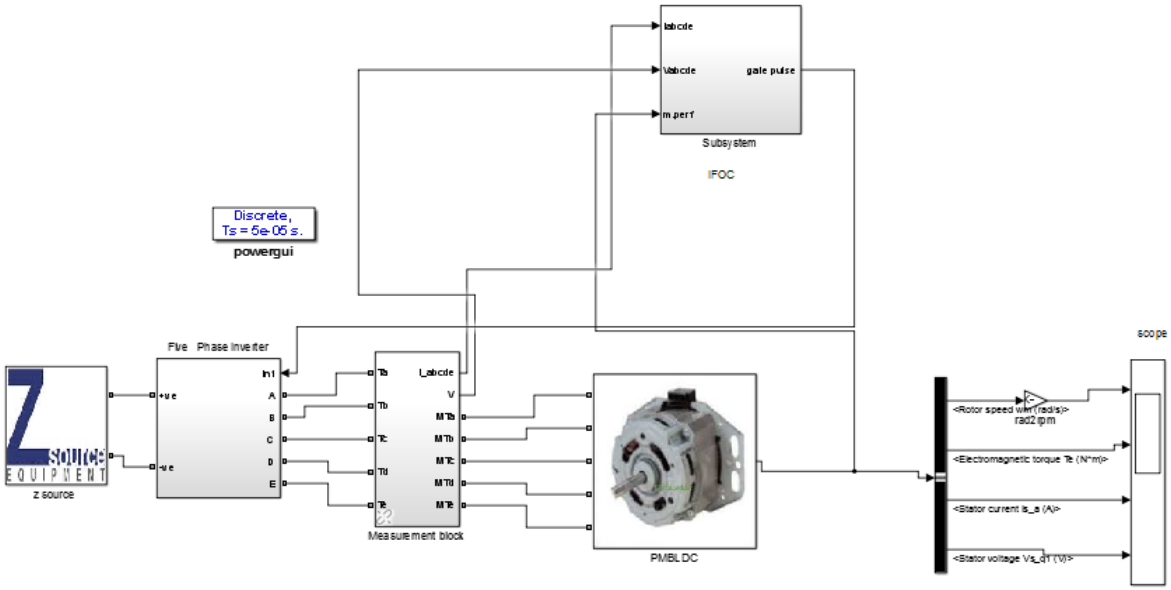

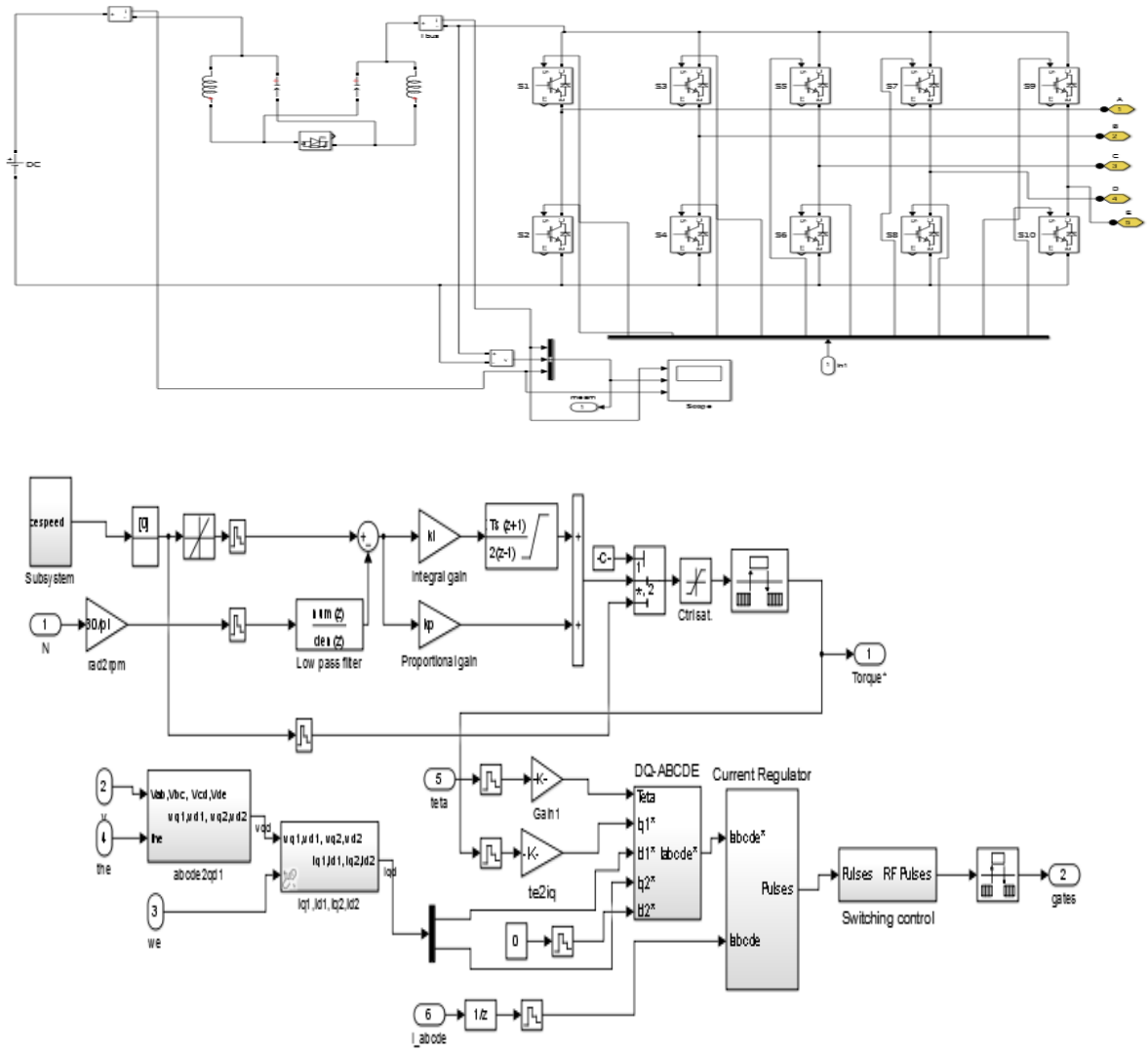

Fig. 7(a) proposed simulation circuit, **(b)** five phase inverter arrangement, **(c)** IFOC controller

The simulation results were considered for 11kW PMBLDC system. Switching frequency and sampling period Ts are 10 kHz and 100 µs respectively. The good performance of estimation can be confirmed for both 1000rpm and 1500rpm. Also, the fast response to step change of speed can be seen through the estimated value. Therefore the following figures should represents varies steady state operations.

Fig.8 shows the results of parameter estimation with overall performance of the proposed system. Also the simulation was performed in two different systems (proposed and conventional) speed at 1000 rpm. Also, these results are categorized as performance during transient and steady state conditions [22]. Fig. 9(a) shows the maximum torque state at 1500 rpm speed condition. Here, the actual torque ripple range should be greater the than the reference torque (7- 12N*m). Ripple minimization of torque waveform is shown in Fig. 9(b).

Table. 2 Simulation Parameter Specifications

Parameter	Value
ZSI parameter	
Inductance	100μH
Capacitance	100μF
Switching Frequency	10 kHz
Five Phase PMSM	
Resistance	1.4 Ω
d-axis inductance	6.6 mH
q-axis inductance	5.8 mH
Stator inductance	6.6 mH
Inertia	0.00176N.m.S^2/rad
Friction Factor	0.000388.m.s/rad
Pole pairs	3
Rated flux	0.1546 Wb

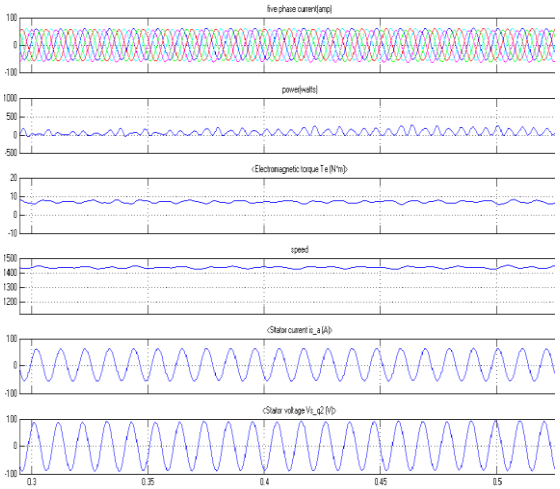

Fig.8 Simulink performance of the PMBLDCM drive at 1400 rpm and rated torque at 10 N*m

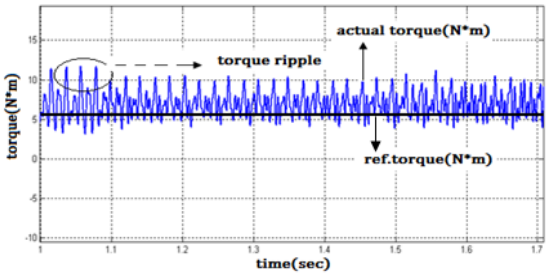

Fig.9 (a) Torque wave form for conventional control system.

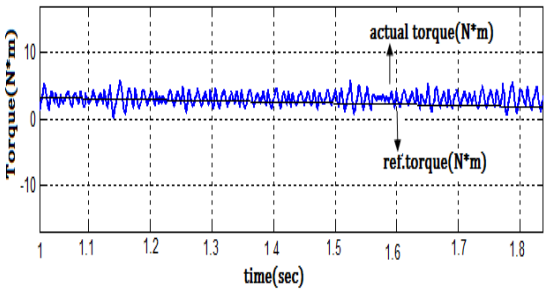

Fig.9 (b) Torque waveform of proposed system.

7. Performances under Transient Condition

Figs. (10-12) show the performance of the drive during speed control of the PMBLDC motor. The reference speed is changed from 750 rpm to 1500 rpm for the rated load performance of the five phases PMBLDC; from 750 rpm to 1000 rpm for the motor at medium rated load; and from 1000 rpm to 1500 rpm for the compressor at maximum rated load. Speed is controlled in fast and smooth at either direction, i.e., acceleration or retardation. Moreover, the stator current of five PMBLDCM is within the allowed limit (twice the rated current) due to the introduction of impedance network in inverter side. Which is allows additional voltage gain by using small shoot through. However, nearly unity power factor is maintained by the drive during these transient conditions.

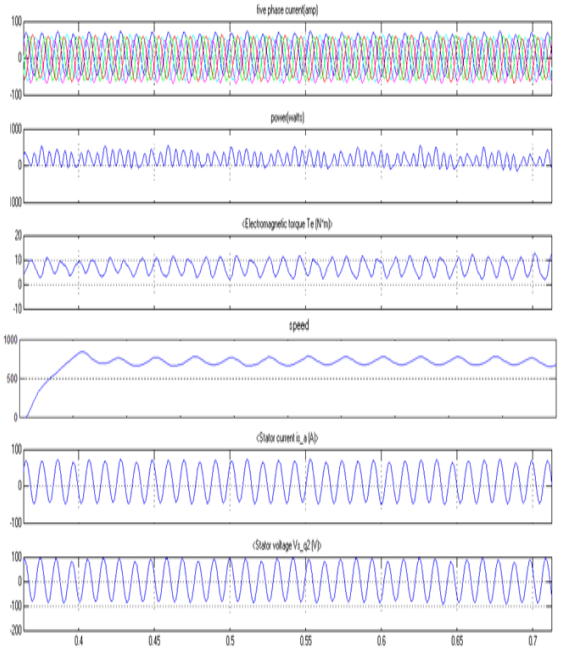

Fig.10 Performance of the PMBLDCM drive under speed 750 rpm

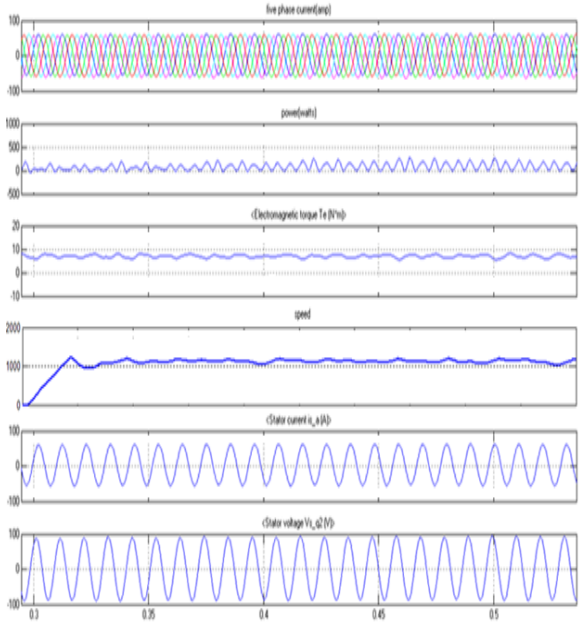

Fig.11 Performance of the PMBLDCM drive under speed 1000 rpm

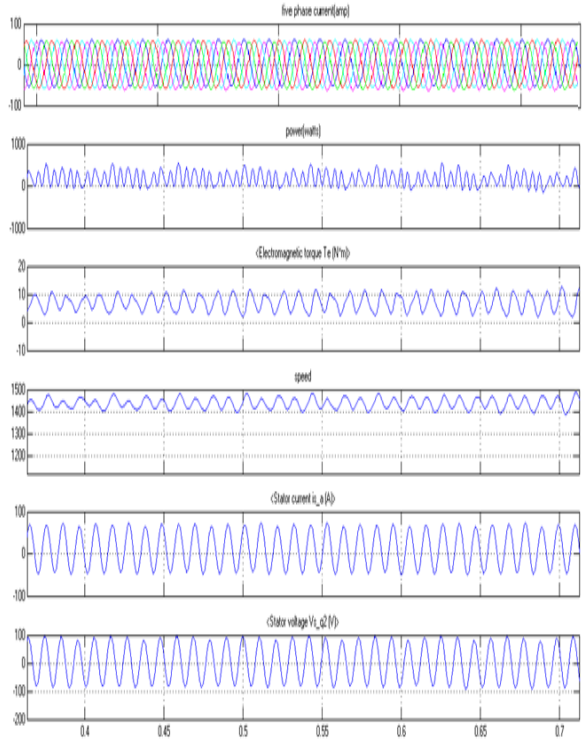

Fig.12 Performance of the PMBLDCM drive under speed 1500 rpm

Fig. 13 and fig. 14 shows The performance of the proposed PMBLDCM drive in terms of various power quality parameters such as THD_i . Reduced THD of the AC mains current are observed in a wide speed range of the PMBLDC motor, Figs.13 & Fig.14 (a-b) shows the conventional current THD waveform for two different speed(1000 rpm & 1500rpm).

Moreover, the proposed THD of the current around 3% along with near unity Power factor in different range of speed (1000 rpm & 1500rpm) and load. Additionally, following current waveforms should show the harmonic content range.

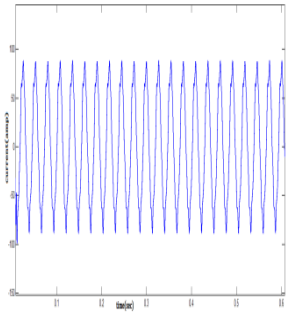

Fig.13(a) conventional waveform for **THD $_i$** at 1000 rpm. **Fig.13(a)** conventional waveform for **THD $_i$** at 1000 rpm.

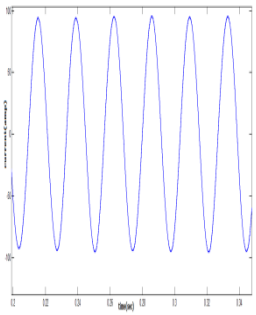

Fig.14(a) Proposed waveform for **THD $_i$** at 1000 rpm

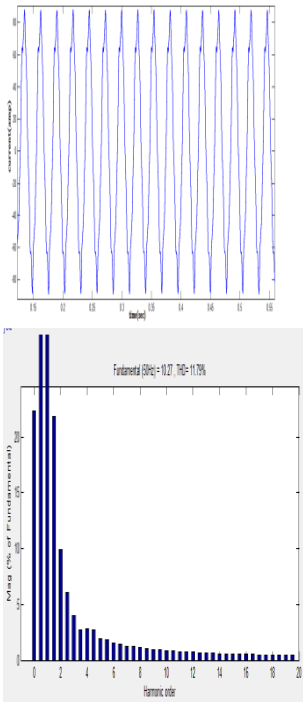

Fig.13(b) conventional waveform-for **THD $_i$** at 1500 rpm.

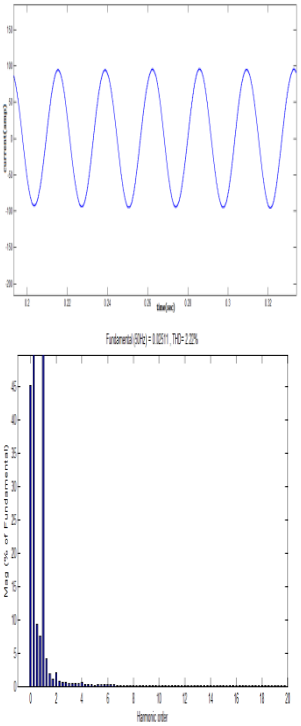

Fig.14 (b) proposed waveform-for **THD $_i$** at 1500 rpm.

Performance evaluation of the proposed PMBLDCM drive is carried out under varying load at rated torque and rated speed. This is demonstrated the operation of the proposed PMBLDCM drive for five phase operation in various practical situations as summarized in Table. 3.

Table.3 Performance under Speed Control At Load Variation

Speed (rpm)	Load (%)	Proposed method		Conventional method	
		THD	η_{Drive} %	THD	η_{Drive} %
750	40	3.68	93.4	22.68	78.5
900	55	3.24	94.6	20	79.9
1000	65	2.96	95.9	19.06	80.9
1200	80	2.60	96.7	17.02	82.6
1400	90	2.33	97.2	14.26	84.2
1600	100	2.02	98	11.76	85.9

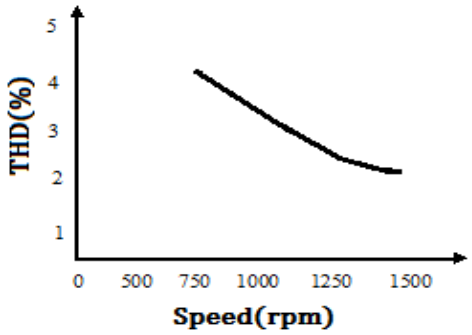

Fig.15(a) Variation of speed and the corresponding THD

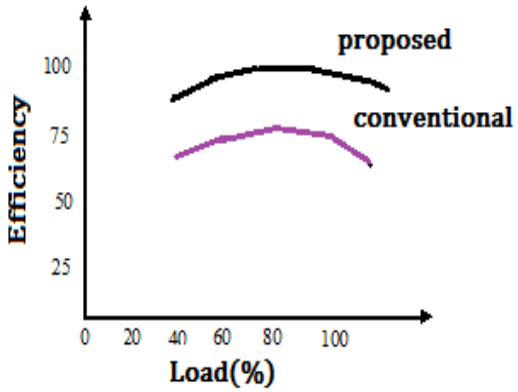

Fig.15(b) Variation of load and the corresponding efficiency.

Figs. 15(a-b) shows variation of speed and THD, load and efficiency is within the specified limits of international norms [23] along with near 3.7% to 2.2% of THD is achieved for wide range of speed. Fig 15(b) shows the efficiency curve for various load condition

8. Conclusion

This paper proposed a multi phase for permanent magnet brushless DC motor to minimize torque ripple. The method combined indirect field oriented control strategy and PWM mode, which avoids the large current and torque ripple. At the same time, in the case when five-phase Z-source inverter 72° conduction mode, improved the given input voltage level and lookup table of switching devices states solved torque ripple in commutation. Finally, simulation results were presented and compared with conventional torque control method. This is provided feasible and effective reduction of torque ripple and voltage saturation of the proposed strategy.

References

1. Zhenguo Li, Songfa Zhang, Shenghai Zhou and Jin-Woo Ahn "Torque Ripple Minimization in Direct Torque Control of Brushless DC Motor" J Electr Eng Technol Vol. 9, No. 5: 1569-1576, 2014.
2. Zhu ZQ, Howe D (2007) Electrical machines and drives for electric vehicle, hybrid and fuel cell vehicles. Proc IEEE Trans 95(4):746–765.
3. E. Levi, "Multiphase electric machines for variable-speed applications,"IEEE Trans. Ind. Electron., vol. 55, no. 5, pp. 1893– 1909, May 2008.
4. Y. Tang, S. J. Xie, C. H. Zhang, and Z. G. Xu, "Improved Z-source inverter with reduced Z-source capacitor voltage stress and soft-start capability," IEEE Trans. Power Electron., vol. 24, no. 2, pp. 409–415, Feb. 2009.
5. Fang Z Peng, Z-Source Inverter, IEEE Transactions on Industry application, Volume 39, No.2,pp:504-510, March/April 2003.
6. Quoc-Nam Trinh, Hong-Hee Lee "A New Z-Source Inverter Topology with High Voltage Boost Ability" Journal of Electrical Engineering & Technology Vol. 7, No. 5, pp. 714~723, 2012.
7. P. C. Loh, F. Gao, and F. Blaabjerg, "Embedded EZ-source inverters," IEEE Trans. Ind. Appl., vol. 46, no. 1, pp. 256–267, Jan./Feb. 2010.
8. Emil Levi, "Multiphase Electric Machines for Variable-Speed Applications", IEEE Transactions on Industrial Electronics, Vol. 55, No. 5, pp.1893-1909, May 2008.
9. M. Mohr, W. T. Franke, B. Wittig, and F. W. Fuchs, "Converter systems for fuel cells in the medium power range—A comparative study," IEEE Trans. Ind. Electron., vol. 57, no. 6, pp. 2024–2032, Jun. 2010.
10. Sanjeev Singh, Bhim Singh, "PFC Bridge Converter for Voltage-controlled Adjustable-speed PMBLDCM Drive," Journal of Electrical Engineering & Technology Vol. 6, No. 2, pp. 215~225, 2011.
11. S. Rajakaruna and L. Jayawickrama, "Steady-State Analysis and Designing Impedance Network of Z-Source Inverters," in IEEE Transactions on Industrial Electronics, vol. 57, no. 7, pp. 2483-2491, July 2010.
12. Kai Deng, Fei Mei, Jun Mei, Jianyong Zheng and Guangxu Fu "An Extended Switched-inductor Quasi-Z-source Inverter," J Electr Eng Technol Vol. 9, No. 2: 541-549, 2014.
13. Leila Parsa and Hamid A. Toliyat, 'sensorless direct torque control of Five-Phase Interior Permanent-Magnet Motor Drives',IEEE transactions on industry applications, vol. 41, no. 4, july/August 2007.

14. Q. Tran, T. Chun, J. Ahn, and H. Lee, "Algorithms for controlling both the DC boost and AC output voltage of Z-source inverter," IEEE Trans. Ind. Electron., vol. 54, no. 5, pp. 2745–2750, Oct. 2007.
15. D.Vinnikov and I. Roasto, "Quasi-Z-source-based isolated DC/DC converters for distributed power generation," IEEE Trans. Ind. Electron.,vol. 58, no. 1, pp. 192–201, Jan. 2011.
16. Y. Zhao and T. A. Lipo, "Space vector PWM control of dual three-phase induction machine using vector space decomposition," IEEE Trans. Ind. Appl., vol. 31, no. 5, pp. 1100–1109, Sep./Oct. 1995.
17. Drazen Dujic, Martin Jones, and Emil Levi, "Analysis of Output Current-Ripple RMS in Multiphase Drives Using Polygon Approach," IEEE Transactions on Power Electronics, vol. 25, no. 7, JULY 2010, pp. 1838 – 1849.